PERGAMON

International Journal of Heat and Mass Transfer 43 (2000) 2101–2115

International Journal of HEAT and MASS TRANSFER

www.elsevier.com/locate/ijhmt

Constructal T-shaped fins

Adrian Bejan*, Majed Almogbel

Department of Mechanical Engineering and Materials Science, Duke University, Durham, NC 27708-0300, USA

Received 30 March 1999; received in revised form 10 September 1999

Abstract

This paper reports the geometric (constructal) optimization of T-shaped fin assemblies, where the objective is to maximize the global thermal conductance of the assembly, subject to total volume and fin-material constraints. Assemblies of plate fins and cylindrical fins are considered. It is shown that every geometric feature of the assembly is delivered by the optimization principle and the constraints. These optimal features are reported in dimensionless terms for this entire class of fin assemblies. Corresponding results are developed for more evolved versions of the T-shaped assembly, namely, the tau-shaped assembly where the free ends of the thinner fins are bent, the tau-shaped assembly that is narrower than the space allocated to it, and the umbrella-shaped construct containing cylindrical fins. The results show that some of the optimized geometrical features are relatively robust, i.e., insensitive to changes in some of the design parameters.

1. Introduction

Constructal theory is the thought that the geometric form visible in natural flow systems is generated by (i.e., it can be deduced from) a single principle that holds the rank of law [1]. The *constructal law* was first stated for open (or flow) systems: "For a finite-size system to persist in time (to live), it must evolve in such a way that it provides easier access to the imposed currents that flow through it". This statement has two parts. First, it recognizes the natural tendency of imposed currents to construct shapes, i.e., paths of optimal access through constrained open systems. The second part accounts for the changes (i.e., improvements) in these paths, which occur in an identifiable direction that is aligned with time itself.

The formulation of the constructal law refers to an open system with imposed through flow. If the system is isolated and initially in a state of internal nonequilibrium, it will create optimal geometric paths for its internal currents. The constructal law then is the statement that the isolated system selects and optimizes its internal structure (the flow paths) to maximize its speed of approach to equilibrium (uniformity, no flow) [2]. The constructal law was conceived as a purely theoretical way of accounting for the billions and billions of natural patterns that have been recognized empirically as "self-organization" and "self-optimization" in systems far from equilibrium.

The constructal optimization of paths for internal currents was first proposed in the context of pure heat conduction [1], with application to the cooling of heat generating electronics in the limit of decreasing dimensions. The constructal method shows us how to minimize geometrically the thermal resistance between a volume and one point, when the total system volume and the volume fraction occupied by high-conductivity "channels" are constrained. The application of this heat transfer

* Corresponding author. Tel.: +1-919-660-5310; fax: +1-919-660-8963.

E-mail address: abejan@duke.edu (A. Bejan).

0017-9310/00/$ - see front matter
PII: S0017-9310(99)00283-5

Nomenclature

a, b	dimensionless parameters, Eqs. (5) and (20)
A	area [m^2]
f, f_*	fractions, Eq. (16)
h	heat transfer coefficient [W m^{-2} K^{-1}]
k	fin thermal conductivity [W m^{-1} K^{-1}]
L	length [m]
m	fin parameter, Eq. (6)
q	heat current [W]
t	thickness [m]
T	temperature [K]
V	volume [m^3]
W	width [m]
y	fraction, Eq. (17)

Greek symbols

ε	small dimensionless number
θ	dimensionless junction temperature, Eq. (9)
ϕ_1	volume fraction of fin material

Subscripts

f	fin material
m	maximized once
mm	maximized twice

Superscript

(˜)	dimensionless variables, Eqs. (4), (10) and (21)

enhancement method to systems with pure conduction showed that the optimized architecture has a tree-shaped skeleton formed by high-conductivity material. The rest of the material fills the interstices, and generates heat at every point of the given volume. The tree of high-conductivity channels captures the heat current generated by the entire volume, and leads it out of the system through the root point of the tree structure. The interstices of the tree channels are equally important: in every optimized volume element there is a perfect balance between the resistance through the low-conductivity

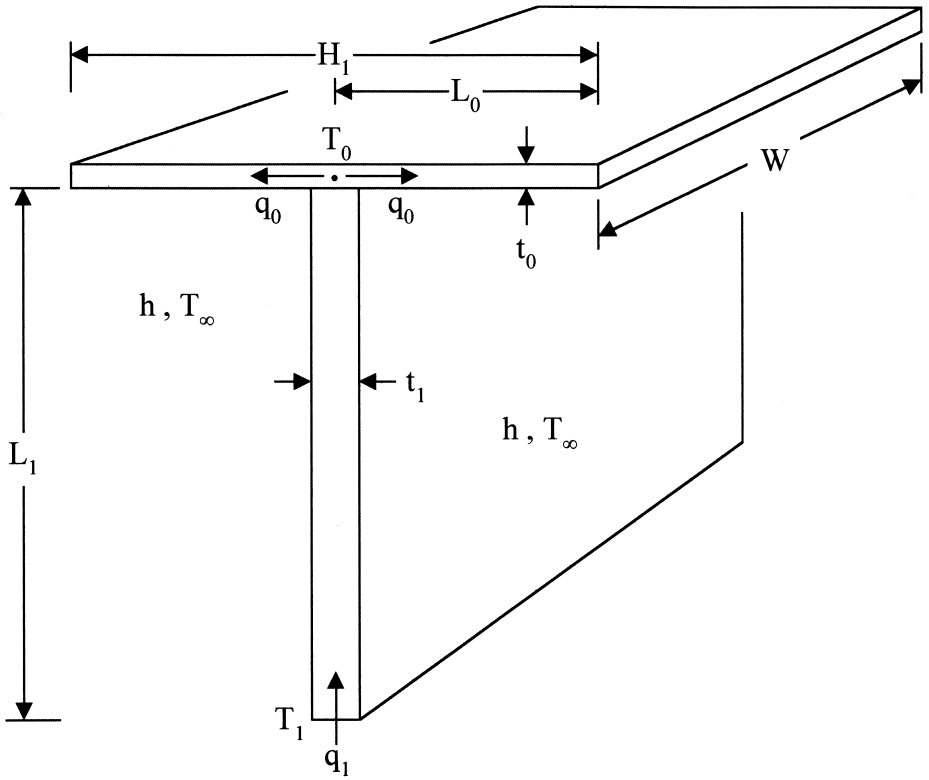

Fig. 1. T-shaped assembly of plate fins.

and high-conductivity materials, i.e., a perfect balance between the two "flow regimes".

The constructal tree is determined completely from one principle: the minimization of global resistance subject to size constraints. Constructal trees have been determined for heat conduction in two dimensions [1] and for fluid flow through a heterogeneous porous medium [3]. The wide applicability of this deterministic principle to the physics of naturally shaped (organized, optimized) flow systems was discussed in a recent review [4].

In this paper we extend the constructal method to a class of systems that transfer heat (between a volume and one point) through a combination of conduction and convection. The system is the assembly of rigidly connected fins that fills a given space, and has a fixed amount of fin material. The heat current (input or output) touches every point of the volume by convection, because the volume is bathed by a steady stream of fluid. This current continues by conduction into the solid links of the fin assembly, and makes contact with the root of the assembly.

Individual fins and assemblies of fins have long been recognized as effective means to augment heat transfer. The literature on this subject is sizeable, as shown by the most current reviews [5,6]. The new aspect that is contributed by the constructal method is the complete geometric optimization of the assembly of fins when the total volume inhabited by the assembly is fixed. In order to illustrate this aspect in the most transparent terms, we apply the constructal method to some of the simplest assembly types that have been recognized in practice [5–10].

2. Unidirectional conduction model

Consider the T-shaped assembly of fins sketched in Fig. 1. Two "elemental" fins of thickness t_0 and length L_0 serve as tributaries to a stem of thickness t_1 and length L_1. The configuration is two-dimensional, with the third dimension (W) sufficiently long in comparison with L_0 and L_1. The heat transfer coefficient h is uniform over all the exposed surfaces. Specified are the temperatures of the root (T_1) and the fluid (T_∞). The temperature at the T junction (T_0) is one of the unknowns, and varies with the geometry of the assembly.

The objective of the following analysis is to determine the optimal geometry $(L_1/L_0, t_1/t_0)$ that is characterized by the maximum global thermal conductance $q_1/(T_1 - T_\infty)$, where q_1 is the heat current through the root section. As in the constructal optimization of conduction trees [1], the present optimization is subjected to two constraints, namely, the total volume (i.e., frontal area) constraint,

$$A = 2L_0L_1 \text{ (constant)} \tag{1}$$

and the fin-material volume constraint,

$$A_f = 2L_0t_0 + t_1L_1 \text{ (constant)} \tag{2}$$

The latter can be expressed as the fin volume fraction $\phi_1 = A_f/A$, which is a constant considerably smaller than 1.

The analysis that delivers the global conductance as a function of the assembly geometry consists of accounting for conduction along the L_0 and L_1 fins, and invoking the continuity of temperature and heat current at the T junction. For each fin we use the unidirectional conduction model, the validity of which is tested later in Eqs. (13) and (14).

For the two elemental fins we used the classical assumptions [5,6,11] and the solution for a fin with non-negligible heat transfer through the tip,

$$\frac{q_0}{kW(T_0 - T_\infty)} = a\tilde{t}_0^{1/2}\frac{\sinh(a\tilde{L}_0\tilde{t}_0^{-1/2}) + (a/2)\tilde{t}_0^{1/2}\cosh(a\tilde{L}_0\tilde{t}_0^{-1/2})}{\cosh(a\tilde{L}_0\tilde{t}_0^{-1/2}) + (a/2)\tilde{t}_0^{1/2}\sinh(a\tilde{L}_0\tilde{t}_0^{-1/2})} \tag{3}$$

where

$$(\tilde{L}_0, \tilde{t}_0) = \frac{(L_0, t_0)}{A^{1/2}} \tag{4}$$

$$a = \left(\frac{2hA^{1/2}}{k}\right)^{1/2} \tag{5}$$

Eq. (3) shows the emergence of the dimensionless parameters $(a, \tilde{L}_0, \tilde{t}_0)$ which influence the dimensionless elemental conductance $q_0/[kW(T_0 - T_\infty)]$. Note the use of $A^{1/2}$ as length scale in the nondimensionalization of the linear dimensions.

The temperature distribution along the stem $T(x)$, from the root ($x = 0$) to the junction ($x = L_1$), is

$$T(x) - T_\infty = (T_1 - T_\infty)\cosh(m_1x) + \left[\frac{T_0 - T_\infty}{\sinh(m_1L_1)} - (T_1 - T_\infty)\frac{\cosh(m_1L_1)}{\sinh(m_1L_1)}\right]\sinh(m_1x) \tag{6}$$

The fin parameter $m_1 = (2h/kt_1)^{1/2}$ can be expressed as $m_1L_1 = a\tilde{L}_1/\tilde{t}_1^{1/2}$. Next, we use $T(x)$ in the equation for the continuity of heat current at the T_0 junction.

$$-kt_1W\left(\frac{\partial T}{\partial x}\right)_{x=L_1} = 2q_0 \tag{7}$$

which can be arranged in the following dimensionless form:

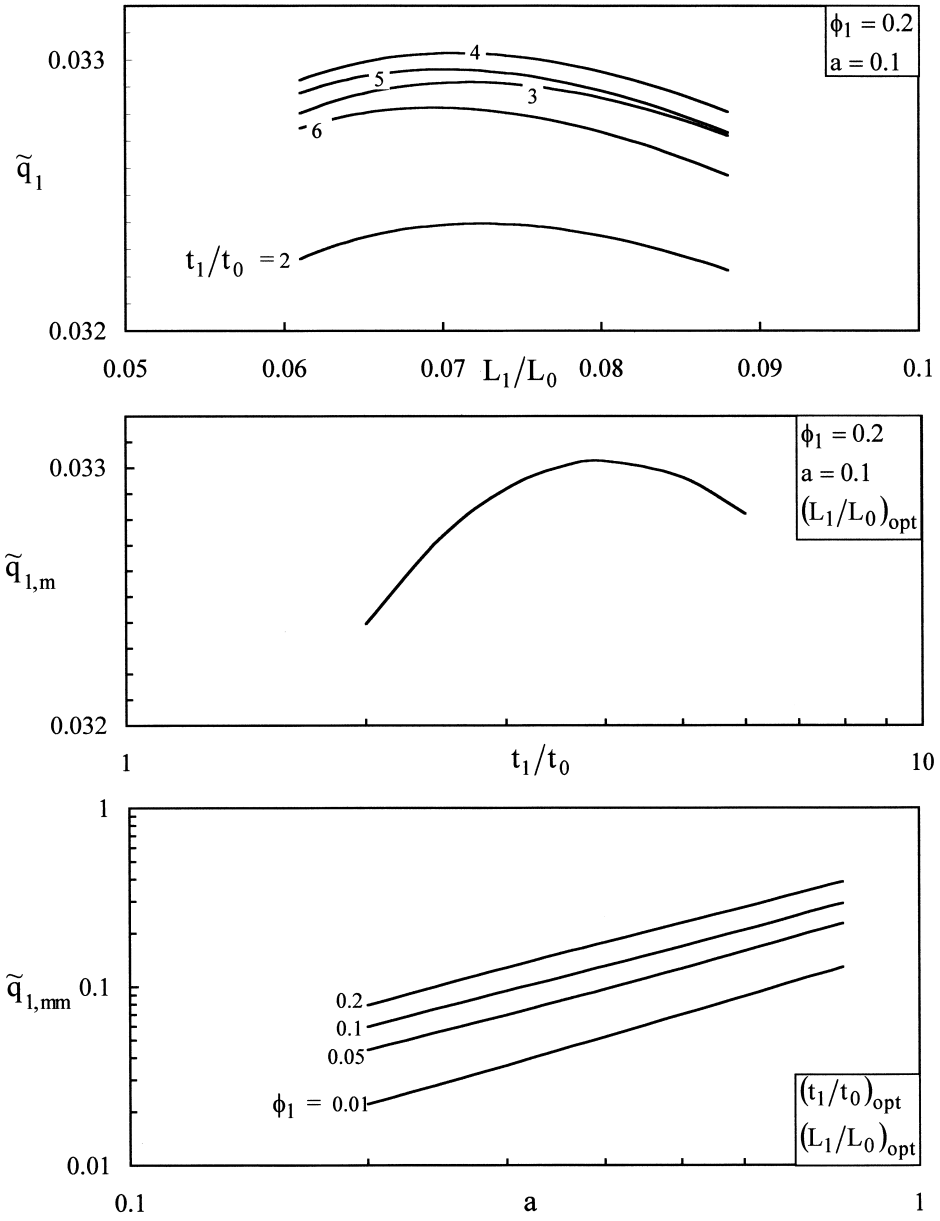

Fig. 2. The double maximization of the overall thermal conductance of the T-shaped construct of Fig. 1.

$$1-\theta\ \cosh(a\tilde{L}_1/\tilde{t}_1^{1/2}) = 2\left(\frac{\tilde{t}_0}{\tilde{t}_1}\right)^{1/2}\theta\ \tanh(a\tilde{L}_0/\tilde{t}_0^{1/2})\sinh(a\tilde{L}_1\tilde{t}_1^{1/2}) \tag{8}$$

Eq. (8) establishes the dimensionless junction temperature as a function of the five dimensionless parameters of the fin assembly,

$$\theta = \frac{T_0 - T_\infty}{T_1 - T_\infty} = \text{function}(a, \tilde{L}_0, \tilde{t}_0, \tilde{L}_1, \tilde{t}_1) \tag{9}$$

Finally, the global thermal conductance is obtained by using Eq. (6) in evaluating the heat current through the root, $q_1 = -kt_1W(\partial T/\partial x)_{x=0}$. The result can be expressed as a dimensionless global conductance,

$$\tilde{q}_1 = \frac{q_1}{kW(T_1 - T_\infty)} = a\tilde{t}_1^{1/2}\frac{\cosh(a\tilde{L}_1/\tilde{t}_1^{1/2}) - \theta}{\sinh(a\tilde{L}_1/\tilde{t}_1^{1/2})}) \tag{10}$$

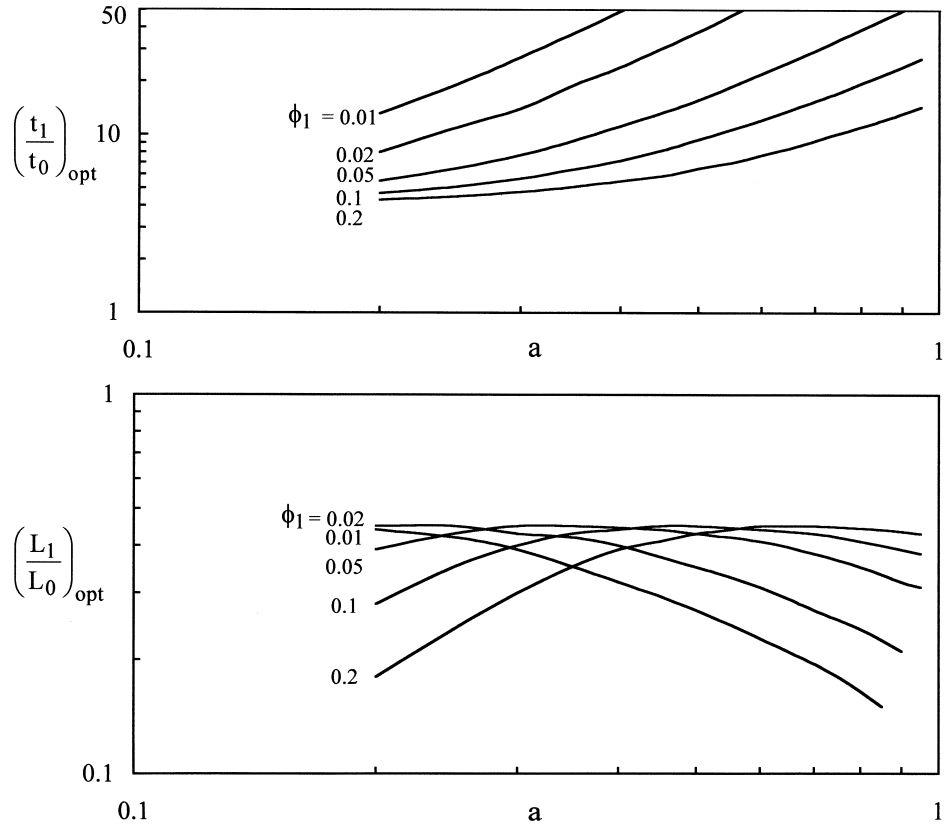

Fig. 3. The optimized geometry of the T-shaped construct of Fig. 1.

for which θ is provided by Eq. (9). The conductance $\tilde{q}_1$ emerges as a function of a, $\tilde{L}_0$, $\tilde{t}_0$, $\tilde{L}_1$ and $\tilde{t}_1$: only three of these parameters are free to vary, because of the volume and fin material constraints (1) and (2), which now read

$$2\tilde{L}_0\tilde{L}_1 = 1 \tag{11}$$

$$\phi_1 = 2\tilde{L}_0\tilde{t}_0 + \tilde{L}_1\tilde{t}_1 \tag{12}$$

In the optimization runs we used t_1/t_0 and L_1/L_0 as degrees of freedom, while assigning discrete values to the parameter a. Fig. 2 shows that $\tilde{q}_1$ can be maximized with respect to both L_1/L_0 and t_1/t_0, i.e., with respect to the external and internal shapes of the fin assembly. In the first frame of the figure the overall conductance is maximized with respect to L_1/L_0 by holding t_1/t_0 constant. The result is the maximized conductance $\tilde{q}_{1,m}$ shown in the second frame. This operation is repeated many times for other values of t_1/t_0, until $\tilde{q}_{1,m}$ can be maximized for the second time. The end result of this double maximization is the conductance $\tilde{q}_{1,mm}$ shown in the third frame: here we also show that we repeated the double maximization procedure for an entire range of a and ϕ_1 values, which are consistent with practical values. For example, in forced convection to gas flow the order of magnitude of h is 10^2 W/m^2 K, while the thermal conductivities of aluminum and copper are of order 10^2 W/m K. Substituting these values and $A^{1/2} \sim 1$ cm in Eq. (5) we obtain $a \sim 10^{-1}$.

3. Optimal T-shaped geometry

Results for the optimal geometry of the T-shaped construct can be generated by using the procedure of

Table 1
Numerical examples of optimized T-shaped fin assemblies ($\phi_1 = 0.086$, $a = 0.185$)

	$\tilde{L}_0$	$\tilde{L}_1$	$\tilde{t}_0$	$\tilde{t}_1$	$\tilde{q}_1$
Constructal	1.33	0.376	0.0194	0.091	0.0516
Kraus [5]	0.71	0.689	0.0191	0.086	0.040

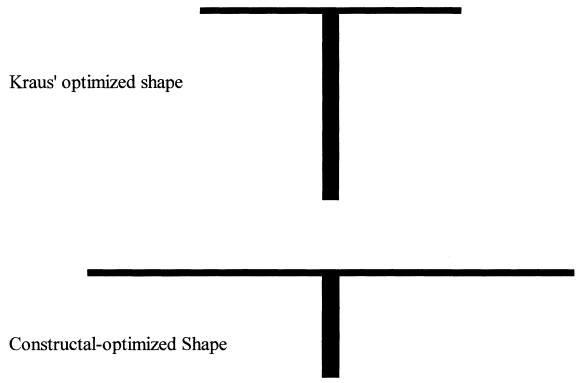

Fig. 4. Examples of optimized T-shaped fin assemblies ($\phi_1 = 0.086$, $a = 0.185$).

Fig. 2 to cover a wider range (a, ϕ_1). In this extensive numerical work it is necessary to keep in mind the range of validity of the unidirectional conduction model on which the analysis is based. The model is valid when the following Biot number criterion is satisfied [12]:

$$\left(\frac{ht_{0,1}}{k}\right)^{1/2} \ll 1 \tag{13}$$

According to this criterion, the two dimensionless thicknesses ($\tilde{t}_0$, $\tilde{t}_1$) must be small enough so that

$$a\left(\frac{\tilde{t}_{0,1}}{2}\right)^{1/2} < \varepsilon \tag{14}$$

where ε is a number smaller than 1. The numerical results described in this paper satisfy the condition (14) with $\varepsilon = 0.1$.

The bottom frame of Fig. 2 shows that the maximized conductance of the T-shaped construct increases as both ϕ_1 and a increase. In the range $0.01 \leq \phi_1 \leq 0.2$ and $0.1 \leq a \leq 1$ these results are correlated within 12% by the power law

$$\tilde{q}_{1,\,\mathrm{mm}} = 0.894 a^{1.08} \phi_1^{0.407} \tag{15}$$

Fig. 3 shows the corresponding results for the optimized geometry of the construct. The internal aspect ratio $(t_1/t_0)_{\mathrm{opt}}$ increases monotonically as a increases and as ϕ_1 decreases; however, these effects are weak when a becomes small and ϕ_1 becomes large. The external aspect ratio $(L_1/L_0)_{\mathrm{opt}}$ has a more interesting behavior when ϕ_1 is fixed: this ratio exhibits a maximum with respect to parameter a. Note that when $(L_1/L_0)_{\mathrm{opt}}$ is known, the individual lengths ($\tilde{L}_{1,\,\mathrm{opt}}$, $\tilde{L}_{0,\,\mathrm{opt}}$) follow immediately from the volume constraint (11). Similarly, when the ratio $(t_1/t_0)_{\mathrm{opt}}$ is known, the individual thicknesses ($\tilde{t}_{1,\,\mathrm{opt}}$ $\tilde{t}_{0,\,\mathrm{opt}}$) can be calculated easily from the material constraint (12).

A numerical example of the optimized structure produced by this method is presented in Table 1 and the lower part of Fig. 4. This example corresponds to a case optimized in an earlier study by Kraus [5] (Fig. 4, top), who used $k = 200$ W/m K, $h = 60$ W/m^2 K and fin lengths and thicknesses that required a total frontal area $A = 32.4$ cm^2 and solid volume fraction $\phi_1 = 0.086$. In this case a = 0.185, cf. Eq. (5). The two designs of Fig. 4 satisfy the unidirectional conduction

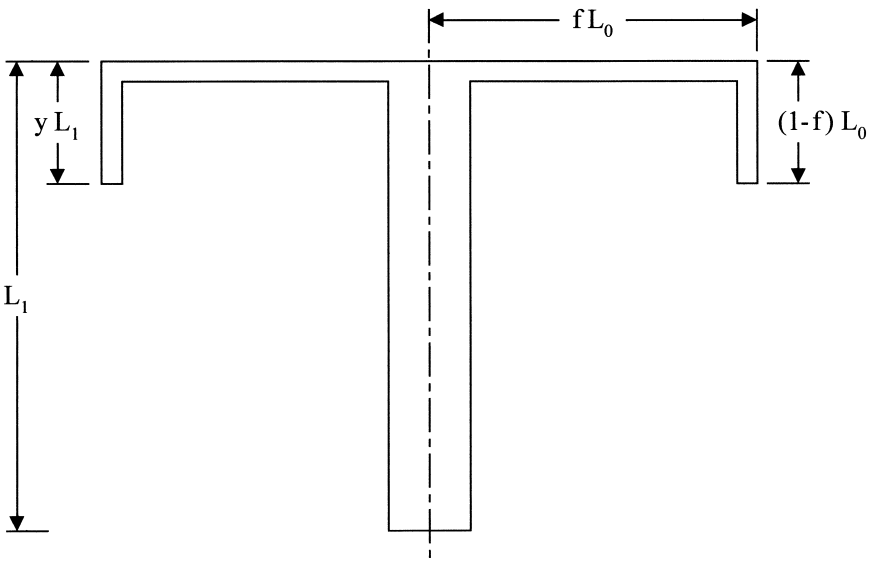

Fig. 5. Tau-shaped assembly of plate fins.

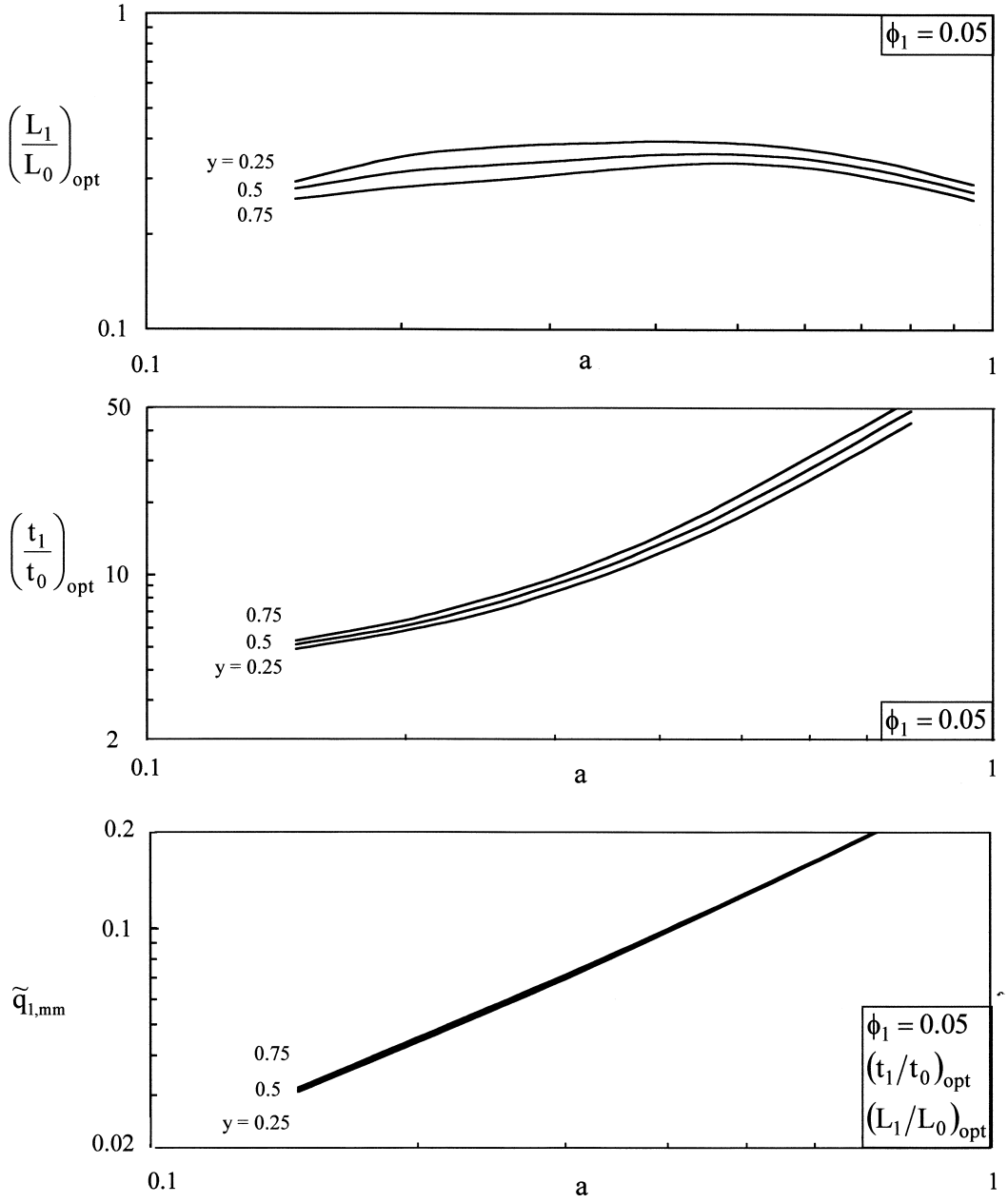

Fig. 6. The optimized geometry and global performance of tau-shaped fin assemblies ($\phi_1 = 0.05$).

criterion (14); in both cases the left side of Eq. (14) has the values $a(t_0/2)^{1/2} = 0.018$ and $a(\tilde{t}_1/2)^{1/2} = 0.04$.

Table 1 shows that the constructal-optimized thicknesses are nearly the same as in Kraus' design, and that the geometric differences result from the fin lengths. In the constructal case the elemental fins (L_0) are considerably longer. The main difference in the constructal design is the 29% increase in the global thermal conductance of the T-shaped assembly.

4. Tau-shaped fin assemblies

The slenderness of the elemental fins in the constructal design (Fig. 4) may turn into a disadvantage if the

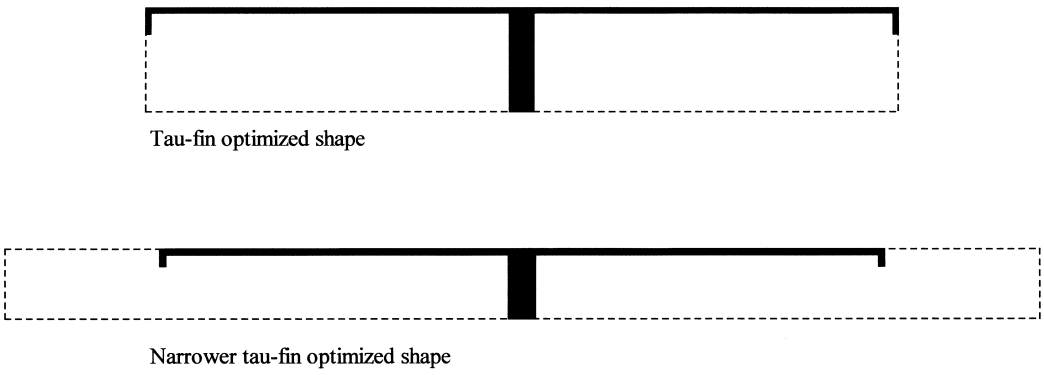

Fig. 7. Optimized tau-shaped constructs for $\phi_1 = 0.086$ and $a = 0.185$.

design is limited by flow induced vibrations. One way of extending the applicability of the constructal approach is to bend the ends of the L_0 fins, as shown in Fig. 5. This technique was also described by Kraus [5]. It is particularly important in the constructal design because the bending of the elemental ends allows the structure to "fill better" its allotted volume. Filling volumes in an optimal way (with objective, or purpose, relative to the use of volume-to-point flows) is the essence of the constructal method.

The bending of the L_0 fins introduces a new dimensionless parameter: the fraction f, such that the turned end is of length $(1-f)L_0$, and the portion that is in thermal contact with the stem is of length fL_0. The frontal area constraint (1) is replaced by $A = 2fL_0L_1$, which means that the dimensionless size constraint is now

$$2f\tilde{L}_0\tilde{L}_1 = 1 \tag{16}$$

The rest of the mathematical apparatus is the same as in Section 3. The new parameter f can take values in the range $f_* < f \leq 1$, where $f = 1$ represents the T-shaped assembly documented in Section 3, and $f_* = 1 - L_1/L_0$ represents the extreme where the bent end would be as long as the stem, $(1-f)L_0 = L_1$. We continue to assume that in each case the fin thickness is considerably smaller than the fin length, and that the unidirectional conduction model [13,14] applies.

The important question for the tau-shaped design is how the f parameter influences the optimal geometry and performance of the assembly. In other words, it is important to determine the thermal-design impact of increasing the stiffness of the assembly. This question is answered in Fig. 6. We used three f values such that the length of the turned end of the L_0 fin is 25, 50 and, finally, 75% of the stem length L_1. Note the graphic definition of the y fraction on Fig. 5, namely $f = 1 - yL_1/L_0$. The T-shaped designs of Fig. 2 correspond to $y = 0$.

The bottom frame of Fig. 6 shows that the overall conductance of the assembly decreases just slightly when the ends of the elemental fins are bent. The optimized aspect ratios $(L_1/L_0)_{\text{opt}}$ and $(t_1/t_0)_{\text{opt}}$ are also relatively insensitive to bending the ends. Fig. 7 shows the optimized "tau" geometry that corresponds to the case of Fig. 4 when $y = 0.25$. This design satisfies the unidirectional conduction criterion (14), because $a(\tilde{t}_0/2)^{1/2} = 0.18$ and $a(\tilde{t}_1/2)^{1/2} = 0.04$.

In conclusion, the optimized geometry and performance of T-shaped fins (Section 3) is "robust", and can be used as a good approximation for tau-shaped constructs that fill the same frontal area. The bending of the elemental fins introduces a small thermal conductance penalty, which may be acceptable in view of the increased stiffness of the assembly.

5. Narrower tau-shaped assemblies

The tau-shaped configuration needs an additional adjustment if several such fins are to be mounted on the same wall (Fig. 8). The uniform-h assumption makes it necessary to leave a space between the bent ends of consecutive elemental fins. This means that the rectangle circumscribed to each "tau" must be somewhat narrower than the volume (frontal rectangular area) allocated and kept constant for that assembly.

In Fig. 8 we chose an end-to-end spacing that equals the spacing between each bent end and its own stem. Since the horizontal portion of the elemental fin has

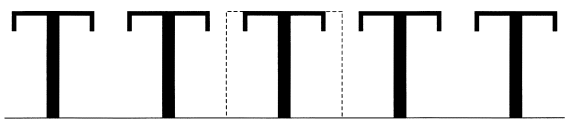

Fig. 8. Narrower tau-shaped constructs mounted on the same wall.

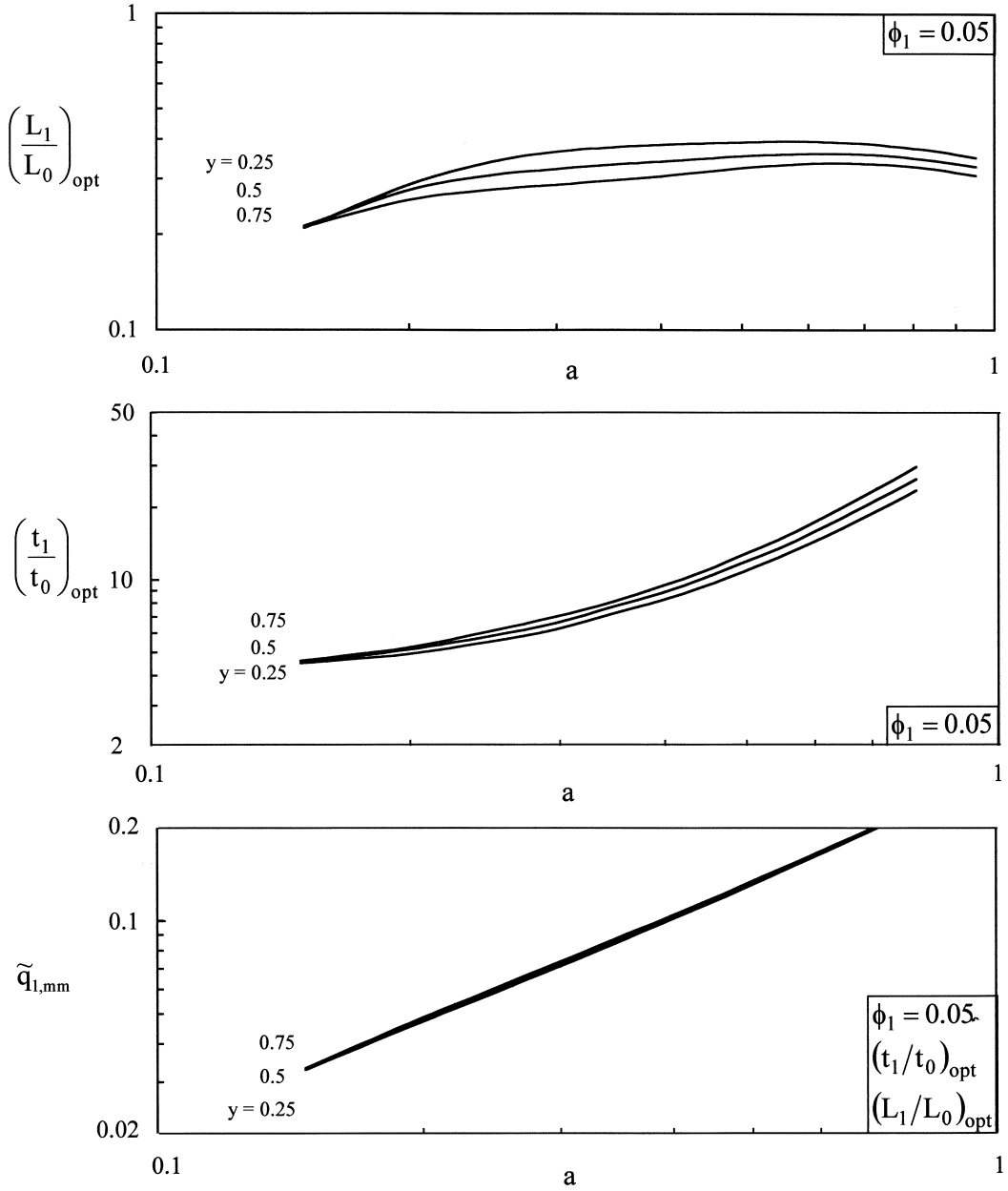

Fig. 9. The optimized geometry and global performance of the narrower tau-shaped assemblies of Fig. 8.

the length $L_0 - yL_1$, the distance from the L_1 stem to the vertical side of the allocated frontal area is $(3/2) \times (L_0 - yL_1)$. The frontal area constraint is $A = 2(3/2)(L_0 - yL_1)L_1$, which assumes the dimensionless form

$$3(\tilde{L}_0 - y\tilde{L}_1)\tilde{L}_1 = 1 \tag{17}$$

Fig. 9 reports the dimensions of the tau-shaped assembly optimized subject to constraint (17). These results were developed for the same parameters as in Fig. 6: their purpose is to show that the new constraint (17) has almost no effect on the optimized dimensions of the assembly.

The same conclusion is drawn from Fig. 7, which compares the shapes of the tau-shaped assemblies optimized subject to constraints (16) and (17). The conduction along the narrower tau-shaped fin shown in Fig. 7

is unidirectional because $a(\tilde{t}_0/2)^{1/2} = 0.02$ and $a(\tilde{t}_1/2)^{1/2} = 0.04$, cf. criterion (14).

The two designs of Fig. 7 occupy the same frontal area (the dashed-line rectangle). The two shapes are nearly the same: the assembly that is narrower than its allocated area (the lower drawing) has a shorter and thicker stem than the assembly that spans the entire width of the area (the upper drawing). The maximized thermal conductances of the top and bottom designs of Fig. 7 are $\tilde{q}_1 = 0.0507$ and 0.0526, respectively. These values indicate slight deterioration in performance relative to the optimized design with straight elemental fins (Table 1, constructal design).

In conclusion, the optimized assembly is robust not only with respect to the bending of the tips of the elemental (L_0) fins, but also with respect to the spacing left between the bent tip and the margin of the frontal flow area allocated to the assembly.

6. Umbrellas of cylindrical fins

The preceding material outlined several classes of results that are generated by a single principle. In this section we consider an additional example of how the method may be applied to a new class of fin-assemblies: the "umbrella" arrangement shown in Fig. 10. A cylindrical fin of length L_1 and diameter D_1 serves as stem for the spokes of the wheel formed by n_1 elemental fins of length L_0 and diameter D_0. The case illustrated in Fig. 10 for $n_1 = 2$. The total space allocated to this construct is the cylinder of radius L_0 and height L_1,

$$V = \pi L_0^2 L_1 \text{ (constant)} \tag{18}$$

The total volume occupied by the fin material is also constrained,

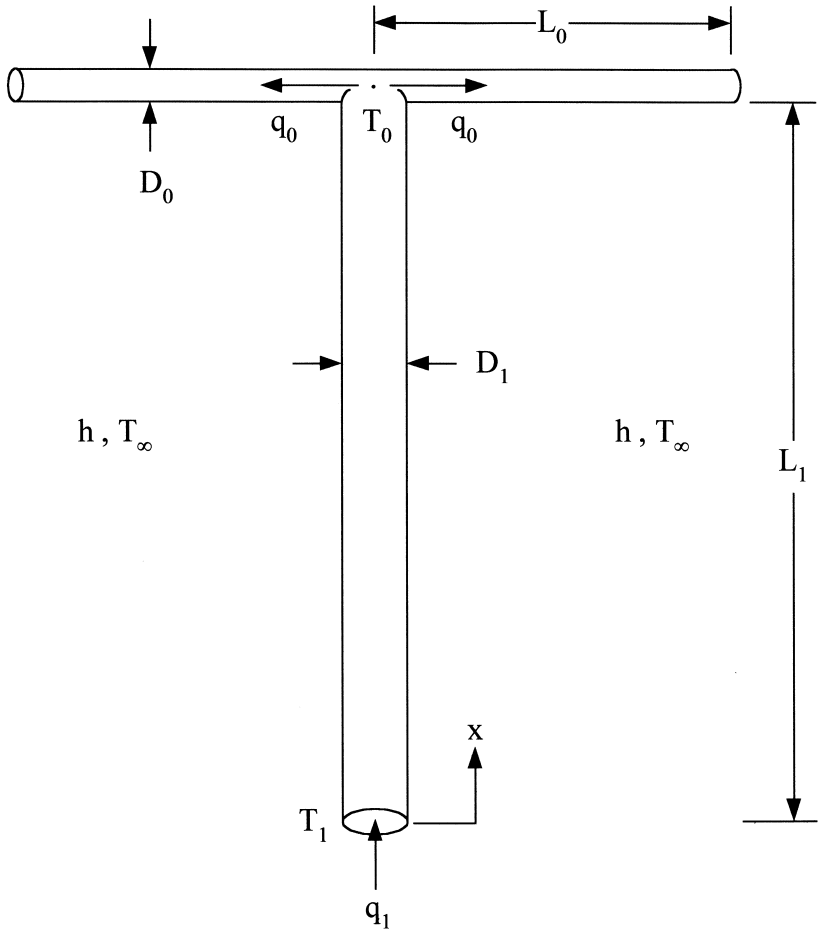

Fig. 10. Umbrella-shaped assembly of cylindrical fins ($n_1 = 2$).

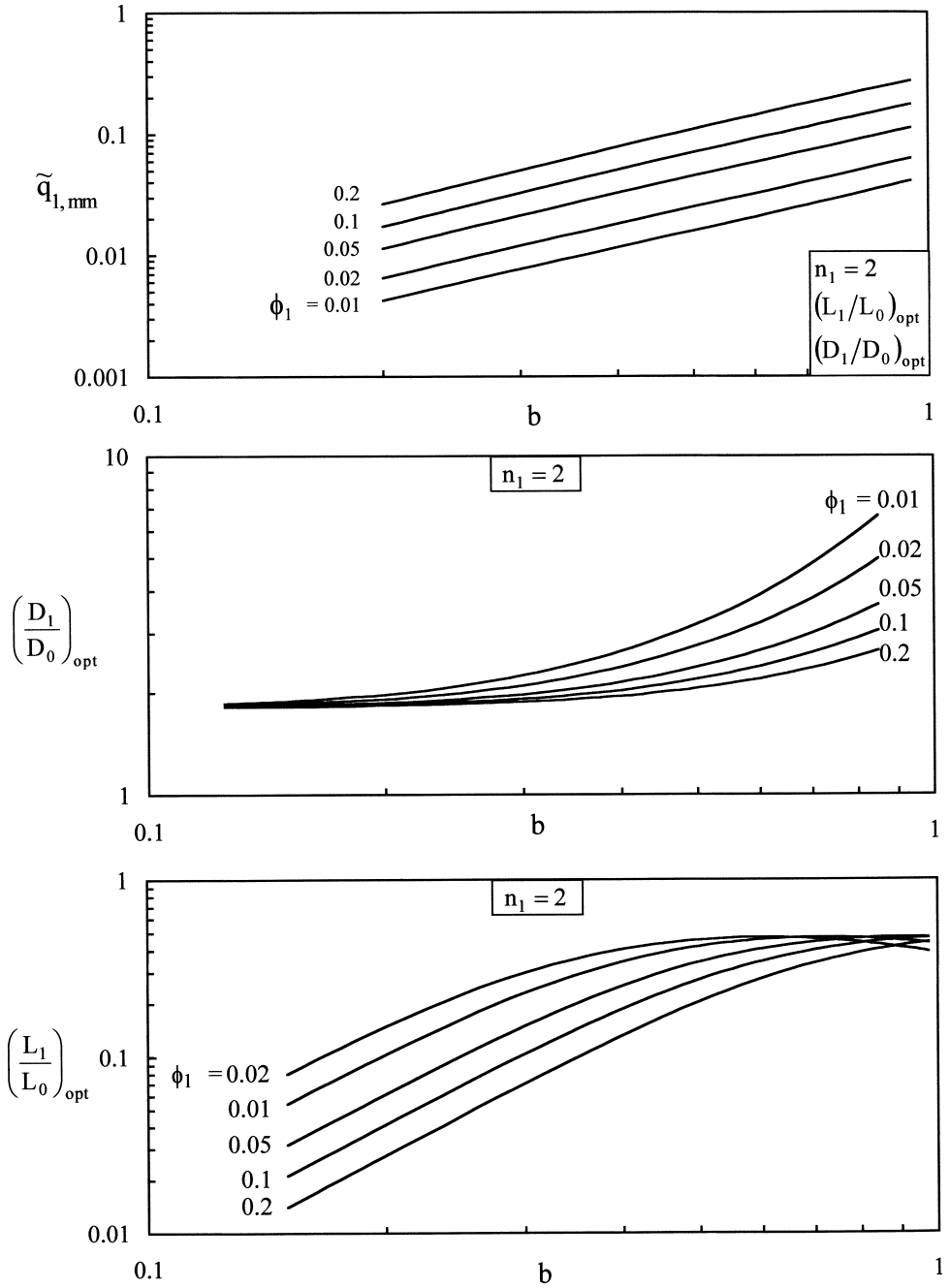

Fig. 11. The optimized geometry and overall thermal conductance of the umbrella construct with $n_1 = 2$.

$$V_f = \frac{\pi}{4} D_1^2 L_1 + n_1 \frac{\pi}{4} D_0^2 L_0 \text{ (constant)} \tag{19}$$

The dimensionless alternative to constraint (19) is the solid volume fraction $\phi_1 = V_f/V$, which is fixed.

The objective is to determine the optimal umbrella geometry such that the global thermal conductance $q_1/(T_1 - T_\infty)$ is maximum. The analysis follows the same steps as in Sections 2 and 3, and is not detailed here. The role of plate thicknesses (t_0, t_1) is now played by the cylinder diameters (D_0, D_1), and the constraints (1) and (2) are replaced by Eqs. (18) and (19). The main step is the continuity of heat current through the

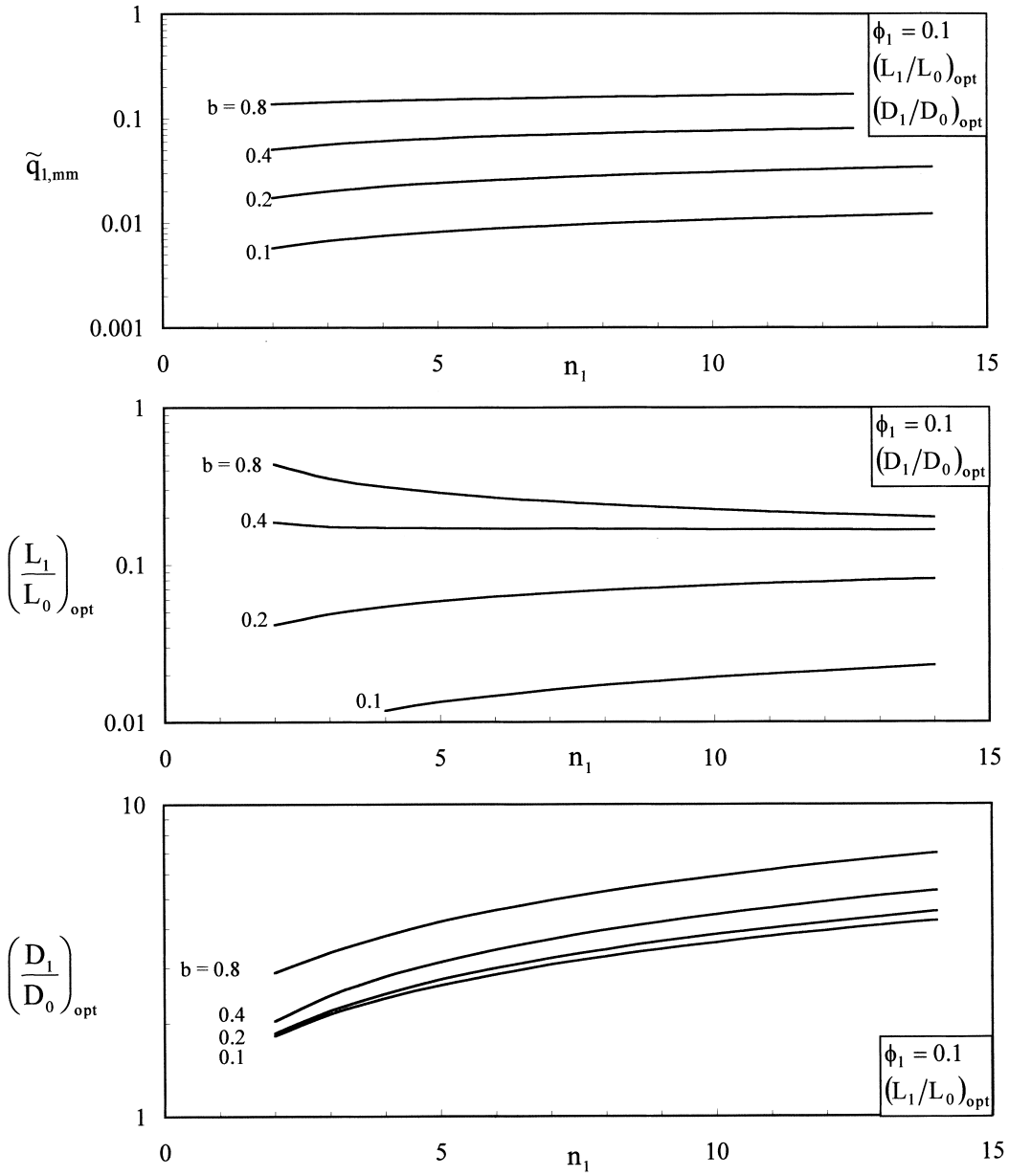

Fig. 12. The effect of the number of spokes n_1 on the optimized geometry and overall thermal conductance of the umbrella construct.

umbrella hub of temperature T_0. We report only the emerging dimensionless groups, and the optimization results. In place of parameter a of Eq. (5) we now have

$$b = \left(\frac{4hV^{1/3}}{k}\right)^{1/2} \tag{20}$$

The dimensionless global conductance definition (10) is replaced by

$$\tilde{q}_1 = \frac{q_1}{kV^{1/3}(T_1 - T_\infty)} \tag{21}$$

The optimized geometry for the case with two spokes is summarized in Fig. 11. The geometry is represented by the aspect ratios $(D_1/D_0)_{opt}$ and $(L_1/L_0)_{opt}$, which are functions of b and ϕ_1. The ratio $(D_1/D_0)_{opt}$

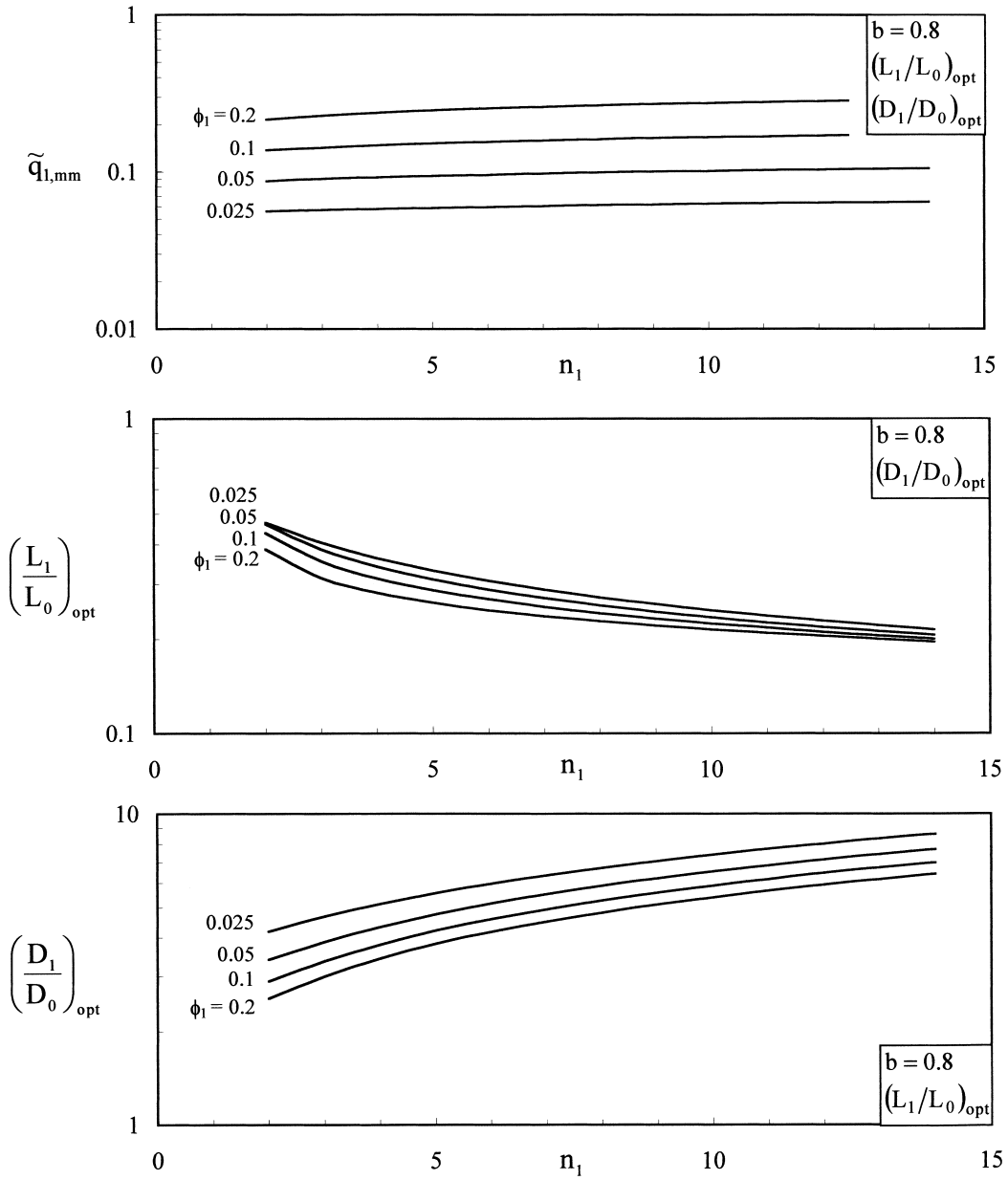

Fig. 12 (*continued*)

approaches 1.82 as b drops below 0.1. The ratio $(L_1/L_0)_{opt}$ is nearly constant (~0.4) when b is of the order of 1. The twice maximized conductance behaves as a power law in both b and ϕ_1; the data of the top frame of Fig. 11 are correlated within 12% by an expression that is quite similar to Eq. (15),

$$\tilde{q}_{1,\,mm} = 0.77 b^{1.47} \phi_1^{0.61} \tag{22}$$

The double optimization procedure (Fig. 11) was repeated for larger n_1 values. The results covering the range $2 \leq n_1 \leq 15$ are reported in Fig. 12a for constant ϕ_1 and varying b, and in Fig. 12b for constant b and varying ϕ_1. In both presentations the effect of n_1 on the twice-maximized conductance is weak. The ratio $(D_1/D_0)_{opt}$ increases as n_1 increases, i.e., the spokes become relatively thinner when they are more numer-

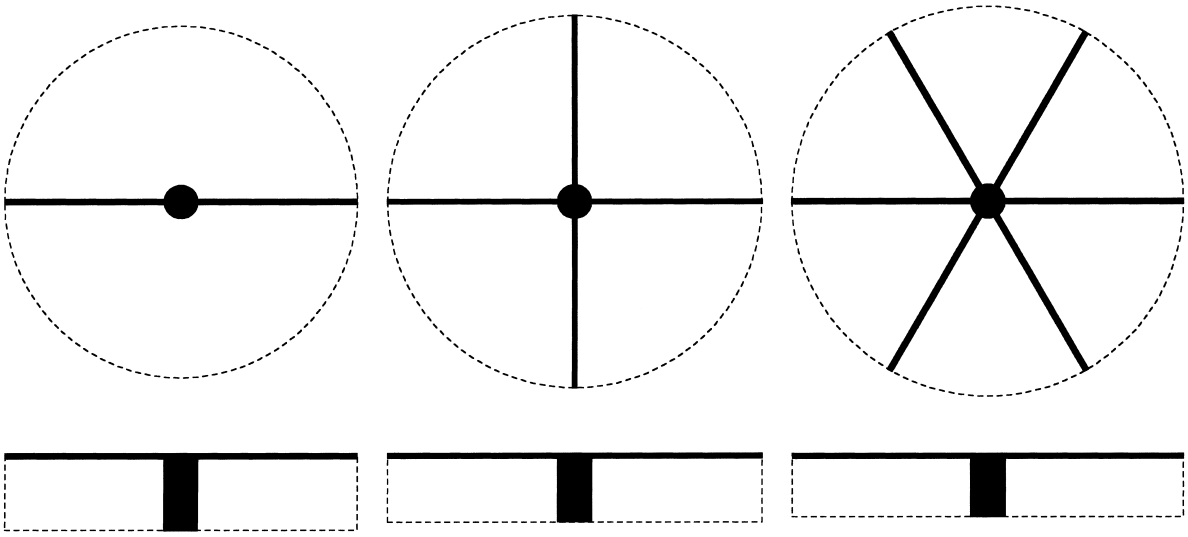

Fig. 13. Examples of optimized umbrella constructs with $\phi_1 = 0.01$ and $b = 0.8$.

ous. The ratio $(L_1/L_0)_{opt}$ is more sensitive to changes in b (Fig. 12a) than to changes in ϕ_1 and n_1.

Fig. 13 shows graphically how the number of spokes influences the optimized geometry. The dashed contour indicates the allocated space (V), which is the same in all three cases. In sum, the optimization of the umbrella construct leads to concrete geometric aspect ratios, and the observation that the optimized geometry is robust with respect to certain parameters. The same conclusion was reached in the two earlier cases treated in this paper.

7. Concluding remarks

The analysis and optimization work presented in this paper showed that the global thermal conductance of fin assemblies can be maximized by geometric optimization subject to total volume and fin material constraints. The optimization and the constraints deliver every geometric feature of the assembly, e.g., Fig. 4 (bottom) and Fig. 7. Noteworthy is the emergence of an optimal external shape for the assembly (e.g., Fig. 2, top) and an internal optimal ratio of plate-fin thicknesses (e.g., Fig. 2, middle).

Three assembly configurations have been optimized. The simplest is the T-shaped assembly of plate fins, for which we showed that the constructal optimization can lead to substantial increases in global conductance relative to current optimal designs that fill the same volume and use the same amount of fin material (e.g., Table 1). Tau-shaped assemblies fill their allotted space better, while exhibiting only a slight decrease in global conductance relative to their T-shaped counterparts (Fig. 6). The paper reports the results for the optimized geometries of all T-shaped, tau-shaped and umbrella-shaped assemblies that conform to the unidirectional heat conduction model. The range covered by these systems is marked by the dimensionless parameters ϕ_1 and a or b. These results may be refined in future studies, for example, by relaxing the classical constant-h assumption.

One useful aspect of the optimized geometries is that certain architectural features are relatively "robust", i.e., insensitive to changes in design parameters. Compare, for example, the two profiles drawn in Fig. 7, which show that the optimized thinner fins are almost the same, regardless of whether they span the entire width of the space allocated to them. Compare also Eqs. (15) and (22). Another example is provided

by the optimized external and internal ratios $((L_1/L_0)_{opt}, (t_1/t_0)_{opt}$; Fig. 6), which do not vary significantly with the lengths of the bent ends of the thinner fins. The feature of robustness was also revealed by the optimized architectures of other tree paths and duct cross-sections produced by the constructal method [4].

The robustness of some of the results, i.e., their weak dependence on some of the constrained design parameters, is also related to the idealizations that have been adopted. An important idealization is the assumption that the heat transfer coefficient is independent of the free flow area shape. Future studies may address the effect of relaxing this assumption on T-assembly architecture. An example of how one may proceed is given in Refs. [13,14], where the heat transfer coefficient was linked to (i.e., derived from) the optimal spacing between adjacent parallel plates. The choice is based on the well known principle of optimizing internal spacings for both forced convection and natural convection [15].

Acknowledgements

The work reported in this paper was supported by the National Science Foundation and the General Organization for Technical Education and Vocational Training, Riyadh, Saudi Arabia.

References

[1] A. Bejan, Constructal-theory network of conducting paths for cooling a heat generating volume, International Journal of Heat and Mass Transfer 40 (1997) 799–816.

[2] N. Dan, A. Bejan, Constructal tree networks for the time-dependent discharge of a finite-size volume to one point, Journal of Applied Physics 84 (1998) 3042–3050.

[3] A. Bejan, M.R. Errera, Deterministic tree networks for fluid flow: geometry for minimal flow resistance between a volume and one point, Fractals 5 (1997) 685–695.

[4] A. Bejan, Advanced Engineering Thermodynamics, 2nd ed., Wiley, New York, 1997.

[5] A.D. Kraus, Developments in the analysis of finned arrays, Donald Q. Kern Award Lecture, National Heat Transfer Conference, Baltimore, MD, August 11, 1997, International Journal of Transport Phenomena, 1 (1999) 141–164.

[6] A. Aziz, Optimum dimensions of extended surfaces operating in a convective environment, Applied Mechanics Reviews 45 (5) (1992) 155–173.

[7] W.R. Hamburgen, Optimal, finned heat sinks, WRL Research Report 86/4, Digital, Western Research Laboratory, Palo Alto, CA, 1986.

[8] D.J. Lee, W.W. Lin, Second-law analysis on a fractal-like fin under crossflow, AIChE Journal 41 (1995) 2314–2317.

[9] W.W. Lin, D.J. Lee, Diffusion-convection process in a branching fin, Chemical Engineering Communications 158 (1997) 59–70.

[10] W.W. Lin, D.J. Lee, Second-law analysis on a pin-fin array under cross-flow, International Journal of Heat and Mass Transfer 40 (1997) 1937–1945.

[11] K.A. Gardner, Efficiency of extended surfaces, Transactions ASME 67 (1945) 621–631.

[12] A. Bejan, Heat Transfer, Wiley, New York, 1993.

[13] A. Alebrahim, A. Bejan, Constructal trees of circular fins for conductive and convective heat transfer, International Journal of Heat and Mass Transfer 42 (1999) 3585–3597.

[14] A. Bejan, N. Dan, Constructal trees of convective fins, Journal of Heat Transfer 121 (1999) 675–682.

[15] A. Bejan, Convection Heat Transfer, 2nd ed., Wiley, New York, 1995 (chapters 3 and 4).